Theoretical and Experimental Study of Medium Effects on the Structure and Spectroscopy of the $[Fe(CN)_5NO]^{2-}$ Ion

Darío A. Estrin,* Luis M. Baraldo, Leonardo D. Slep, Beatriz C. Barja, and José A. Olabe*

Departamento de Química Inorgánica, Analítica y Química-Física and INQUIMAE, Facultad de Ciencias Exactas y Naturales Universidad de Buenos Aires, Ciudad Universitaria-Pab II, 01428 Buenos Aires, Argentina

Luca Paglieri and Giorgina Corongiu

Centro di Ricerca, Sviluppo e Studi Superiori in Sardegna (CRS4), P.O. Box 1048, 09100 Cagliari, Italy

Received September 15, 1995[⊗]

The influence of the solvent on the structure and IR spectrum of the $[Fe(CN)_5NO]^{2-}$ ion is investigated by using gradient corrected density functional theory. IR spectra are also measured on different solvents and the results obtained are compared with the predicted ones. We have treated the solvent effects with a continuum model, based on the Onsager's reaction field approach; in order to mimic strong specific interactions, calculations were also performed on the complex protonated at the cyanide trans to the nitrosyl group. The reaction field calculations predict only qualitatively the most important observed trends, e.g., the shifts in the nitrosyl stretching wavenumber, but fail in accounting quantitatively for the differences between the spectra in water and acetonitrile. The possible role of specific interactions is consistently accounted for by interpreting the experimental shifts of the NO stretching wavenumber ν(NO), as well as the visible absorption energies, when changing the Lewis acidity of the solvent, as measured by the Gutmann's acceptor number. Ligand population analysis was performed to relate the solvent effects with the σ donor and π acceptor behavior of cyanide and nitrosyl ligands. The significance of ν(NO) shifts as a result of changes in the medium is discussed in view of the physiological relevance of transition-metal nitrosyl chemistry.

Introduction

Density functional theory (DFT) has proved to be a powerful and economical tool for the study of a variety of molecular properties in coordination compounds.[1−4] However, the calculations rely on the assumption that the molecule is perfectly isolated. This is a severe limitation, since most relevant chemical processes involving these compounds are performed in a condensed phase.

The methods formulated to study the solvent effects can be divided in three categories. The first one uses molecular force fields,[5,6] with Monte Carlo or molecular dynamics algorithms. These techniques are very useful when good quality ab-initio derived (or empirical) potentials are available; nevertheless, since rigid parameters are usually used for both solute and solvent, mutual polarization effects are neglected, and this can lead to some misleading results. Moreover, the method cannot either deal with excitation processes or chemical reactions.

The second approach replaces the explicit solvent molecules with a continuum having the appropriate bulk dielectric constant.[7−10] The properties of the continuum solvent represent an average over solvent configurations. The success of dielectric continuum models in dealing with intra- and intermolecular charge-transfer processes in solution is well recognized, as long as specific solvent effects such as hydrogen bonding or other donor−acceptor interactions are absent.[11,12]

In the third approach, the effects of the medium are modeled by introducing a small number of solvent molecules together with the solute in the quantum-chemical calculation and treating the entire system as a supermolecule; the drawback of this methodology is that the computational expense grows rapidly with the number of solvent molecules considered.

The chemistry of transition metal cyanide complexes containing one or several ancillary L ligands has been fully explored.[13] In the series of pentacyano-L complexes,[14] the coordination chemistry of the L = nitrosyl derivatives is now a special target,[15,16] in view of the renewal of interest in the still unraveled

[⊗] Abstract published in *Advance ACS Abstracts,* May 15, 1996.

(1) Salahub, D. R.; Fournier, R.; Mlynarski, P.; Papai, I.; St-Amant, A.; Ushio, J. In *Theory and Applications of Density Functional Approaches to Chemistry*; Labanowski, J., Andzelm, J., Eds.; Springer-Verlag: Berlin, 1990.
(2) Ziegler, T. *Chem. Rev.* **1991**, *91*, 651.
(3) Sosa, C.; Andzelm, J.; Elkin, B. C.; Wimmer, E.; Dobbs K. D.; Dixon, D. A. *J. Phys. Chem.* **1992**, *96*, 6630.
(4) Andzelm, J.; Wimmer, E. *J. Chem. Phys.* **1992**, *96*, 1280.
(5) Allen, M. P.; Tildesley, D. J. *Computer Simulations in Liquids*; Oxford University Press: London, 1987.
(6) Corongiu, G.; Aida, M.; Pas, M. F.; Clementi, E. In *MOTECC, Modern Techniques in Computational Chemistry*; Clementi, E., Ed.; Escom: Leiden, 1991.
(7) Tapia, O.; Goscinski, O. *Mol. Phys.* **1975**, *29*, 1653.
(8) (a) Wong, M. W.; Frisch, M. J.; Wiberg, K. B. *J. Am. Chem. Soc.* **1991**, *113*, 4476. (b) Wong, M. W.; Wiberg, K. B.; Frisch, M. J. *J. Am. Chem. Soc.* **1992**, *114*, 523. (c) Wong, M. W.; Wiberg, K. B.; Frisch, M. J. *J. Am. Chem. Soc.* **1992**, *114*, 1645.
(9) (a) Tomasi, J.; Bonaccorsi, R.; Cammi, R.; Olivares del Valle, F. J. *TEOCHEM* **1991**, *234*, 401. (b) Miertius, S.; Scrocco, E.; Tomasi, J. *Chem. Phys.* **1990**, *55*, 117.
(10) (a) Cramer, C. J.; Truhlar, D. G. *J. Am. Chem. Soc.* **1993**, *115*, 8810. (b) *J. Comput. Chem.* **1992**, *13*, 1089.
(11) (a) Sullivan, B. P. *J. Phys. Chem.* **1989**, *93*, 24. (b) Creutz, C. *Inorg. Chem.* **1987**, *26*, 2995. (c) Kober, E. M.; Sullivan, B. P.; Meyer, T. J. *Inorg. Chem.* **1984**, *23*, 2098. (d) Goldsby, K. A.; Meyer, T. J. *Inorg. Chem.* **198**, *23*, 3002.
(12) (a) Kolling, O. W. *J. Phys. Chem.* **1991**, *95*, 3950. (b) Powers, M. J.; Meyer, T. J. *J. Am. Chem. Soc.* **1980**, *102*, 1289.
(13) Sharpe, A. G. *The Chemistry of Cyano Complexes of the Transition Metals*; Academic Press: New York, 1976.
(14) Macartney, D. H. *Rev. Inorg. Chem.* **1988**, *9*, 101.

S0020-1669(95)01202-X CCC: $12.00

role of NO in diverse physiological processes.[17] The available evidence suggests that the coordination ability of NO to transition-metal centers (among which the d^6, Fe(II) species with porphyrinic-like coligands such as guanylate cyclase are particularly relevant), as well as the redox interconvertibility of NO to its reduced and/or oxidized forms, appears as a significant aspect of this interesting chemistry. We presently suggest that the interaction with the solvent medium should also be taken into special account in the chemistry of cyanide or cyanide-nitrosyl containing species. The existence of strong environmental intramolecular effects on the bonding in metal-pentacyano-nitrosyl complexes has been recognized.[18] Intermolecular perturbations associated with the presence of countercations or hydrogen bonding effects have also been documented,[19,20] but, however, their influence on the changes in the relevant structural and spectroscopic parameters is still not well understood.

In the present work, the solute−solvent interactions in the pentacyanonitrosylferrate(II) ion, $[Fe(CN)_5NO]^{2-}$, are investigated. First, a DFT approach is employed to calculate structural and IR spectroscopic parameters for the isolated anion in vacuo, as well as in continuum solvent media with $\epsilon = 35.9$ and $\epsilon = 78.5$ (corresponding to acetonitrile and water, respectively). The latter results are contrasted with experimental IR and UV−visible data obtained in different solvents, in order to check the validity of the dielectric continuum model. DFT calculations are extended to the (trans)cyanide-protonated species, in a tentative approach to account for the specific interaction of $[Fe(CN)_5NO]^{2-}$ with the solvent.

Computational Methodology

The calculations in this study are based on the Molecole-DFT program.[21] The Kohn−Sham self-consistent procedure is applied for obtaining the electronic density and energy through the determination of a set of one-electron orbitals.[22] Gaussian basis sets are used for the expansion of the one-electron orbitals and also for the additional auxiliary set used for expanding the electronic density. Matrix elements of the exchange-correlation potential are calculated by a numerical integration scheme.[23] The orbital and auxiliary basis sets optimized by Sim et al.[24] for DFT calculations are used for C, N, O, and H atoms. For Fe, we used the basis set given in ref 25. The contraction patterns are (5211/411/1) for C, N, and O, (4333/431/41) for Fe, and (41/1) for H. For the electronic density expansion sets the contraction patterns are (1111111/111/1) for C, N, and O, (1111111111/111/111) for Fe, and (111111/1) for H. A more detailed description of the technical aspects of the program is given in ref 21.

Computations are performed at the gradient-corrected DFT level. The correlation part is composed by the parametrization of the homogeneous electron gas due to Vosko,[26] with the gradient corrections due to Perdew.[27] The expression due to Becke[28] for the gradient corrections in the exchange term is used.

The Onsager reaction field model[7,8] with a spherical cavity is used, and the solvent is considered as a uniform dielectric, characterized by a given dielectric constant ϵ. The dipole of the solute induces a dipole (reaction field) in the solvent, which in turn interacts with the molecular dipole. The reaction field is updated iteratively until self-consistency is achieved. The cavity radii are calculated quantum-mechanically.[8b] This involves computing the 0.001-au electron density envelope (in the isolated molecule) and scaling by 1.33 in order to obtain an estimation of the molecular volume. Finally, 0.5 Å has been added to the obtained radius a_0, to take into account the nearest approach of solvent molecules.

First derivatives are obtained analytically in the presence of the reaction field. Geometry optimizations are performed by a quasi-Newton minimization method, keeping the cavity size fixed during the optimization process.

Wavenumbers are calculated by numerical differentiation of the analytical energy gradients. Infrared absorption intensities are also evaluated by taking the numerical derivatives of the dipole moment with respect to the nuclear coordinates and then transforming the derivatives to the corresponding ones with respect to the normal modes.

Experimental Procedure

Tetrabuthylammonium (TBA) salts of $[Fe(CN)_5NO]^{2-}$ were prepared by cation exchange (from the Na salt), in a Sephadex SP-25 column, previously equilibrated with TBA chloride. The salts were dried in desiccator over P_2O_5. TBA salts were used for preparing solutions in water, acetonitrile, methanol and acetone, isopropyl alcohol, and DMSO. All the IR spectra were recorded interferometrically between 4000 and 800 cm^{-1} with a 510-P Nicolet Fourier transform infrared spectrometer and a TGS-CsI detector. The attenuated total reflection (ATR) technique was used. The internal reflection element was a 45° ZnSe crystal mounted on a horizontal through plate, allowing the samples to be poured directly on the crystal, without pretreatments. The cell compartment was purged with dry air during the scanning. A reference spectrum was subtracted from that of the sample, both previously ratioed against the empty cell. The resolution was 4 cm^{-1}, with a gain set to 2 and Happ Genzel apodization.

UV−visible spectra were obtained with a Hewlett-Packard HP 8452A diode array spectrophotometer using 10-mm quartz cells. The solvents were saturated with dry argon and transferred into the spectrophotometric cell under Ar atmosphere.

Results and Discussion

Calculations were performed for the isolated complex ($\epsilon = 1$), for the complex immersed in a continuum with dielectric constants of $\epsilon = 35.9$ and $\epsilon = 78.5$, corresponding to those of acetonitrile and water, respectively, and for the complex protonated at the cyanide group trans to the NO. In all the cases, a full geometry optimization and normal mode analysis were performed.

Figure 1 shows the optimized structure for $[Fe(CN)_5NO]^{2-}$ in vacuo. In Table 1 we report the geometrical parameters for all the calculations, compared with X-ray results for $Na_2[Fe(CN)_5NO]\cdot 2H_2O$.[29] The overall agreement with the experimental results is reasonably good, considering that distortions from the gas phase (or solution) are likely to be present in the

(15) (a) McCleverty, J. A. *Chem. Rev.* **1979**, *79*, 53. (b) Bottomley, F. In *Reactions of Coordinated Ligands*; Braterman, P. S., Ed.; Plenum: New York, 1989; Vol. 2, p 115.
(16) Baraldo, L. M.; Bessega, M. S.; Rigotti, G. E.; Olabe, J. A. *Inorg. Chem.* **1994**, *33*, 5980 and references therein.
(17) Stamler, J. S.; Singel, D. J.; Loscalzo, J. *Science* **1992**, *258*, 1898.
(18) Fenske, R. F.; DeKock, R. L. *Inorg. Chem.* **1972**, *11*, 437.
(19) Fairey, M. B.; Irving, R. J. *Spectrochim. Acta* **1964**, *20*, 1757.
(20) Gans, P.; Sabatini, A.; Sacconi, L. *Inorg. Chem.* **1966**, *5*, 1877.
(21) Estrin, D. A.; Corongiu, G.; Clementi, E. In *METECC, Methods and Techniques in Computational Chemistry*; Clementi, E., Ed.; Stef: Cagliari, 1993; Chapter 12.
(22) Kohn, W.; Sham, L. J. *Phys. Rev.* **1965**, *A140*, 1133.
(23) Becke, A. D. *J. Chem. Phys.* **1988**, *88*, 1053.
(24) (a) Sim, F.; Salahub, D. R.; Chin, S.; Dupuis, M. *J. Chem. Phys.* **1991**, *95*, 4317. (b) Sim, F.; St-Amant, A.; Papai, I.; Salahub, D. R. *J. Am. Chem. Soc.* **1992**, *114*, 4391.
(25) Andzelm, J.; Radzio, E.; Salahub, D. R. *J. Comput. Chem.* **1985**, *6*, 520.
(26) Vosko, S. H.; Wilk, L.; Nusair, M. *Can. J. Phys.* **1980**, *58*, 1200.
(27) Perdew, P. W. *Phys. Rev.* **1986**, *B33*, 8800; Erratum, *Ibid*. **1986**, *B34*, 7406.
(28) Becke, A. D. *Phys. Rev.* **1988**, *A38*, 3098.
(29) Bottomley, F.; White, P. S. *Acta Crystallogr.* **1979**, *B35*, 2193.

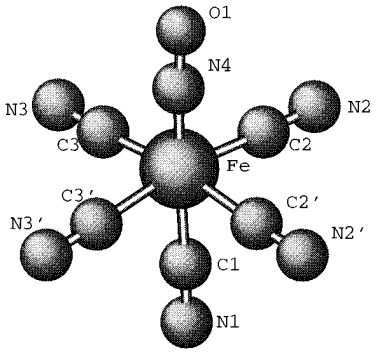

Figure 1. Structure of $[Fe(CN)_5NO]^{2-}$ ion in vacuo.

Table 1. Structural Parameters (Å and deg) for the $[Fe(CN)_5NO]^{2-}$ Anion

parameter	$\epsilon = 1$	$\epsilon = 35.9$	$\epsilon = 78.5$	prot complex	exptl[a]
r(FeC1)	1.949	1.956	1.959	1.865	1.918
r(FeC2)	1.948	1.951	1.954	1.948	1.928
r(FeC2′)	1.948	1.951	1.954	1.948	1.928
r(FeC3)	1.960	1.960	1.957	1.950	1.936
r(FeC3′)	1.960	1.960	1.957	1.952	1.936
r(FeN4)	1.652	1.656	1.654	1.654	1.653
r(C1N1)	1.180	1.182	1.182	1.175	1.150
r(C2N2)	1.181	1.181	1.182	1.178	1.153
r(C2′N2′)	1.181	1.181	1.182	1.178	1.153
r(C3N3)	1.182	1.182	1.182	1.178	1.152
r(C3′N3′)	1.182	1.182	1.182	1.178	1.152
r(N4O1)	1.170	1.164	1.164	1.157	1.125
r(N1H)				1.009	
∠(FeN4O1)	177.1	179.3	179.6	178.8	175.6
∠(FeC1N1)	178.4	178.7	178.6	179.1	179.7
∠(FeC2N2)	177.3	178.9	179.1	179.3	177.9
∠(FeC3N3)	176.3	176.4	176.7	179.6	176.7
∠(C1FeN4)	177.8	179.8	179.7	178.8	176.8
∠(C1FeC2)	83.8	83.7	83.6	83.6	84.3
∠(C1FeC3)	85.0	85.5	85.5	83.4	84.8
∠(C2′FeC2)	89.8	88.6	88.4	88.9	90.0
∠(C2FeC3)	168.8	169.1	169.1	166.9	169.1
∠(C2′FeC3′)	168.8	169.1	169.1	167.9	169.1
∠(C2FeC3′)	88.8	89.6	89.6	89.4	88.7
∠(C2′FeC3)	88.8	89.6	89.6	89.3	88.7
∠(C3FeC3′)	90.4	90.1	90.3	89.6	90.7
∠(N4FeC2)	94.7	96.2	96.2	97.1	93.5
∠(N4FeC3)	96.5	94.6	94.7	96.0	97.4
∠(C1N1H)				172.3	

[a] Reference 29.

solid state. The effects of the solid state environment on the geometry can be very important, for example, in the related system $[Fe(CN)_6]^{4-}$, the DFT predicted structure is octahedral (Fe−C and C−N bond distances 1.976 and 1.197 Å, respectively),[30] while probably due to interactions with countercations and water molecules, the X-ray experimental geometry in $Na_4[Fe(CN)_6]\cdot 10H_2O$ is not (Fe−C and C−N bond distances 1.89, 1.916 and 1.879 and 1.17, 1.18, and 1.19 Å, respectively).[31]

The geometrical parameters show almost no deviations from the isolated complex values in both reaction field and protonated-complex calculations. It can also be seen that reaction field predicted structures for $\epsilon = 35.9$ and $\epsilon = 78.5$ are almost identical. The most sensitive parameter is the NO bond length, which goes from 1.170 Å in the isolated complex to 1.164 Å for the reaction field calculations and to 1.157 Å in the protonated complex.

There has been some controversy regarding the nature of the highest occupied molecular orbital (HOMO) of the $[Fe(CN)_5NO]^{2-}$ complex. The SCCC-MO calculation by Manoharan and Gray[32] predicted the HOMO to be largely of metal character, while more sophisticated semiempirical methods, INDO and SINDO, predicted it to be mainly located on CN equatorial ligands and to be of mixed metal−CN character, respectively.[33,34] The present DFT calculation predicts the HOMO to be mainly located on the metal, but with an important contribution of equatorial cyanides. All previous calculations indicate that the lowest unoccupied molecular orbital (LUMO) is mainly located on the nitrosyl ligand, with some metal contribution.[32−34] The present DFT calculation is in agreement with these results. The nature of the HOMO and LUMO is only slightly affected by changing the dielectric constant. According to these results, the lowest energy band in the UV−visible spectrum could be qualitatively assigned as a metal to ligand charge transfer (MLCT) transition.

A normal mode analysis was performed in the situations mentioned above. The calculated vibrational wavenumbers, IR intensities, and the assignment of the most significant bands are shown in Table 2, which also includes experimental results with samples in the solid state,[35] as well as in aqueous and other solvent media. The error in the optimized geometry is probably the major source of discrepancies between the harmonic vibrational frequencies calculation and the IR experimental results. A possible way to deal with this source of error is to perform the calculation of the vibrational frequencies using the experimental geometry as a reference.[36] However, in this situation the experimental solid state structure is probably not a good reference geometry for the isolated ion. It should also be kept in mind that the theoretical frequencies neglect the effects of anharmonicity.

Figure 2 displays the predicted IR spectra. Table 2 shows that the experimental ν(NO) values are nearly the same for the solid dihydrate and for the aqueous solution, while ν(CN) shows a decrease, which is greater for the axial mode. On the other hand, a significant decrease in ν(NO) is observed upon dehydration, or upon dissolution in a dipolar aprotic solvent, acetonitrile; in the latter conditions, the ν(CN) values remain approximately unchanged, or decrease slightly.

It is well-known that ν(NO) is sensitive to medium effects; thus, different alkaline and alkaline-earth hydrated salts of $[Fe(CN)_5NO]^{2-}$ show different values in the range 1965−1940 cm^{-1}.[35,37−45] A shift to lower wavenumbers of ca. 20−40 cm^{-1} has been measured for cesium, calcium, and strontium pentacyanonitrosyl salts on dehydration,[43,45,46] as with the sodium salt,[35] but no explanation has been given for these systematic

(30) Estrin, D. A.; Hamra, Y.; Paglieri, L.; Slep, L. D.; Olabe, J. Manuscript in preparation.
(31) Gentil, L. A.; Navaza, A.; Olabe, J. A.; Rigotti, G. E. *Inorg. Chim. Acta* **1991**, *179*, 89.
(32) Manoharan, P. T.; Gray, H. B. *Inorg. Chem.* **1966**, *5*, 823.
(33) Bottomley, F.; Grein, F. *J. Chem. Soc. Dalton Trans.* **1980**, 1359.
(34) Wasielewska, E. *Inorg. Chim. Acta* **1986**, *113*, 115.
(35) Paliani, G.; Poletti, A.; Santucci, A. *J. Mol. Struct.* **1971**, *8*, 63.
(36) Berces, A.; Ziegler, T. *J. Phys. Chem.* **1995**, *99*, 11417.
(37) Vergara, M. M.; Varetti, E. L. *Spectrochim. Acta* **1993**, *49A*, 527.
(38) Khanna, R. K.; Brown, C. W.; Jones, L. H. *Inorg. Chem.* **1969**, *8*, 2195.
(39) Amalvy, J. I.; Varetti, E. L.; Aymonino, P. J.; Castellano, E. E.; Piro, O. E.; Punte, G. *J. Cryst. Spectrosc. Res.* **1986**, *16*, 537.
(40) Amalvy, J. I.; Varetti, E. L.; Aymonino, P. J. *J. Phys. Chem. Solids* **1985**, *46*, 1153.
(41) Vergara, M. M.; Varetti, E. L. *J. Phys. Chem. Solids* **1987**, *48*, 13.
(42) Amalvy, J. I.; Varetti, E. L.; Aymonino, P. J. *An. Asoc. Quim. Argent.* **1986**, *74*, 437.
(43) Rigotti, G.; Aymonino, P. J.; Varetti, E. L. *J. Cryst. Spectrosc. Res.* **1984**, *14*, 517.
(44) Varetti, E. L.; Aymonino, P. J. *Inorg. Chim. Acta* **1973**, *7*, 59.
(45) Della Vedova, C. O.; Lesk, J. H.; Varetti, E. L.; Aymonino, P. J.; Piro, O. E.; Rivero, B. E.; Castellano, E. E. *J. Mol. Struct.* **1981**, *170*, 241.

Table 2. Calculated Selected Wavenumbers (cm^{-1}) and IR Intensities (km mol^{-1}) for the $[Fe(CN)_5NO]^{2-}$ Anion in a Continuum; Comparison with Experimental Values[f]

mode		$\epsilon = 1$	$\epsilon = 35.9$	$\epsilon = 78.5$	prot[a]	exptl[b]	exptl[c]	exptl[d]	exptl[e]
$\nu 1$	C−N ax s	2125 (28)	2116 (51)	2116 (50)	2091 (234)	2174 (m)	2164	2155	2145
$\nu 2$	C−N eq s	2121 (6)	2120 (3)	2118 (1)	2143 (0)	2157 (m)			
$\nu 3$	C−N eq s	2115 (112)	2115 (166)	2113 (174)	2139 (47)	2143 (s)	2156	2143	2135
$\nu 4$	C−N eq s	2115 (126)	2114 (169)	2113 (174)	2138 (48)	2143 (s)			
$\nu 5$	C−N eq s	2109 (8)	2101 (19)	2101 (14)	2128 (53)	2161 (m)			
$\nu 6$	N−O s	1853 (928)	1866 (1423)	1869 (1441)	1906 (1002)	1940 (vs)	1918	1937	1892
$\nu 7$	Fe−N s	679 (3)	673 (11)	675 (11)	666 (23)	652 (m)			
$\nu 8$	Fe−N−O b	644 (29)	652 (47)	652 (48)	653 (44)	663 (m)			
$\nu 9$	Fe−N−O b	641 (29)	645 (48)	645 (48)	650 (44)	663 (m)			

[a] The protonated complex also shows a NH stretching band at 3735 cm^{-1}. [b] Results for Na_2 $[Fe(CN)_5NO]\cdot 2H_2O$, ref 35. [c] Results for Na_2 $[Fe(CN)_5NO]$, ref 35. [d] Present work. Results for aqueous solution. [e] Present work. Results for acetonitrile solution. [f] The results for $\nu(CN)_{eq}$ in cases *c*, *d*, and *e* correspond to an unresolved band. b = bending, s = stretching, eq = equatorial, ax = axial, m = medium, s = strong, vs = very strong.

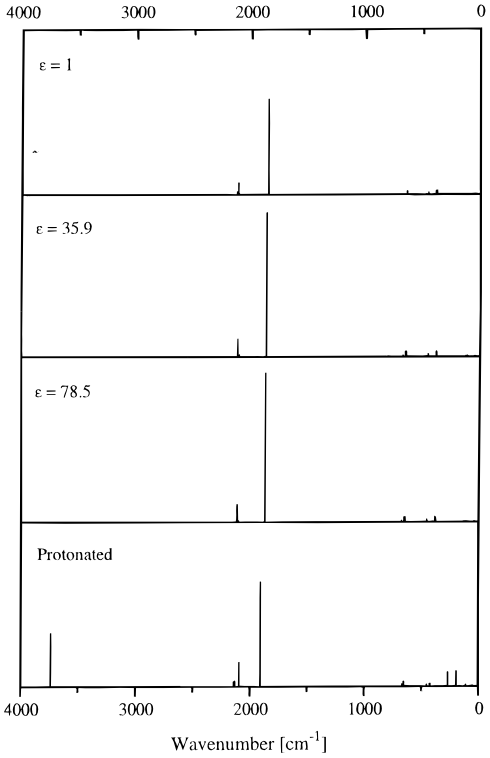

Figure 2. Predicted IR spectra. Calculations for $\epsilon = 1$, $\epsilon = 35.9$, $\epsilon = 78.5$, and protonated complex.

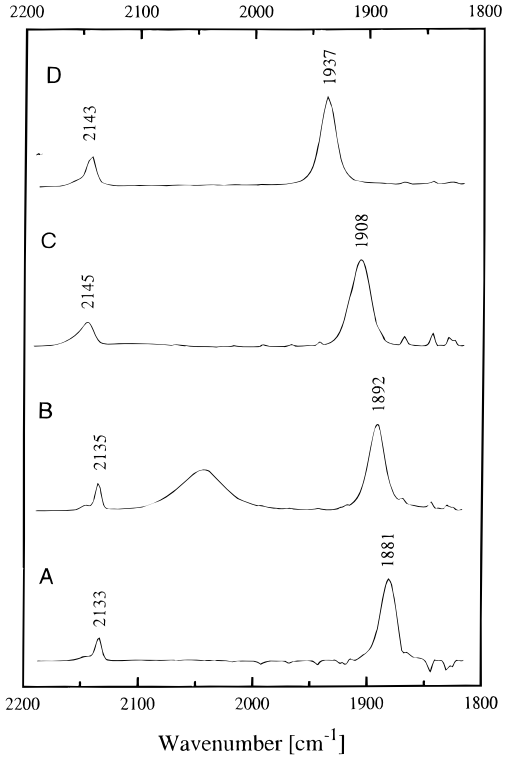

Figure 3. IR spectra of $(TBA)_2$ $[Fe(CN)_5NO]$. ν(NO) and ν(CN) for different solvents. A = acetone; B= acetonitrile; C = methanol; D = water.

results. Moreover, the anhydrous tetrabuthylammonium salt shows an even lower ν(NO) value, 1908 cm^{-1}.[20] In contrast, an upward shift (1952 cm^{-1}) was measured for the nitroprussic acid, $(H_3O)_2$ $[Fe(CN)_5NO]H_2O$,[47] compared to the value found for the solid sodium dihydrate.

In view of the sensitivity of ν(NO) to medium effects, we measured the IR spectra in different solvents. Figure 3 shows the results, with emphasis on the changes observed for ν(CN) and ν(NO). It can be seen that ν(NO) but not ν(CN) values are highly influenced by the solvent.

An empirical approach for dealing with specific solute−solvent interactions is due to Gutmann.[48] Relative donor DN and acceptor AN numbers are defined to describe the solvent's Lewis base and acid character, respectively. By measuring different properties (such as MLCT, metal-to-ligand charge transfer absorption energies, or redox potentials for the metal redox couple), linear plots were obtained against the solvent's AN numbers for a series of $Fe^{II}(CN)_5$ L^{n-} complexes (with L = pyridinic or pyrazinic derivatives).[49] The magnitude of the solvent effect can be expressed by eq 1:

$$\nu_i^s = \nu_i^0 + a_i \mathrm{AN} \qquad (1)$$

where ν_i^s is the measured wavenumber (MLCT band) for a complex *i* in a solvent *s*, and ν_i^0 is the extrapolated wavenumber for a solvent of AN 0. The parameter a_i measures the sensitivity of the complex *i* to the acceptor properties of the solvents. For the series of $M(CN)_xL_{6-x}$ complexes (M = Fe, Ru),[49,50] it was shown that a_i increases with the number of cyanide groups, although a dependence of L was also found. The solute acts as a Lewis base and a solvent of large AN

(46) Vergara, M. M.; Varetti, E. L.; Rigotti G.; Navaza, A. *J. Phys. Chem. Solids* **1989**, *50*, 951.
(47) Varetti, E. L.; Vergara, M. M.; Rigotti, G.; Navaza, A. *J. Phys. Chem. Solids* **1990**, *51*, 381.
(48) Gutmann, V. *The Donor-Acceptor Approach to Molecular Interactions*; Plenum: New York, 1980; *Electrochim. Acta* **1976**, *21*, 661.
(49) (a) Toma, H. E.; Takasugi, M. S. *J. Solution Chem.* **1983**, *12*, 547. (b) Toma, H. E.; Takasugi, M. S. **1989**, *18*, 575.
(50) Timpson, C. J.; Bignozzi, C. A.; Sullivan, B. P.; Kober, E. M.; Meyer, T. M. Private communication.

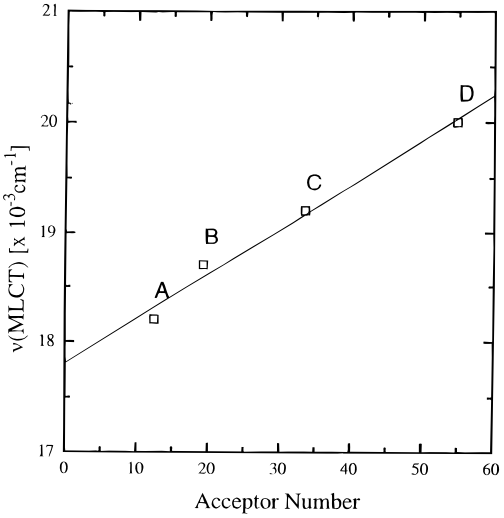

Figure 4. Plot of ν(MLCT), lowest energy visible band of $(TBA)_2[Fe(CN)_5NO]$, against solvent acceptor number (AN). A = acetone; B = DMSO; C = isopropyl alcohol; D = water.

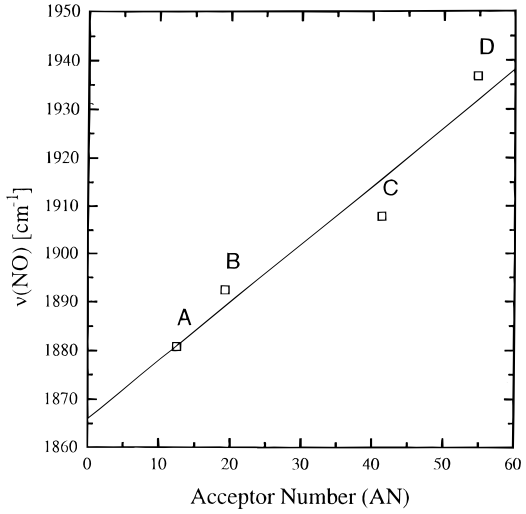

Figure 5. Plot of IR stretching wavenumber ν(NO) against solvent acceptor number (AN) (Gutmann's scale). A = acetone; B= acetonitrile; C = methanol; D = water.

stabilizes preferentially the complex ground state by removing π-electron density from the cyanide ligands and increasing π-back-bonding with the metal ion. As the MLCT excitation involves an electron being largely transferred from the M(II) center out to the L ligand (thus the metal becomes M(III)), the basicity at the cyanides in the excited state will be lower than in the ground state; consequently, the energy separation between the metal donor (dπ) and ligand acceptor (π*) orbitals will increase proportionately, leading to hypsochromic shifts in the CT bands as a function of AN.

Figure 4 shows the plot of ν(MLCT) for the $[Fe(CN)_5NO]^{2-}$ ion (lowest energy MLCT visible band) against AN. By comparison with the results for the $[Fe(CN)_5pz]^{3-}$ complex (pz = pyrazine) which shows a slope of $a = 101$ (consistent with a pentacyanide species),[49] it can be seen that the nitrosyl complex shows an apparently anomalously low value, $a = 41$. As shown previously,[49] a decrease in a can be traced to additional solvation of the L ligand, but the magnitude of the effect on the nitrosyl complex could be hardly associated to this interaction, which seems to be weak indeed (see below). Instead, we assign the decrease in a to the strong electron-withdrawing influence of the NO^+ ligand, which decreases the basicity at the cyanide ligands and, therefore, the sensitivity toward solvent interactions.

Figure 5 shows a linear correlation of the infrared stretching wavenumber, ν(NO), with AN = 0. The ν(NO) value decreases for lower AN; remarkably, the extrapolated value for AN 0 is 1866 cm^{-1}, which compares well with the DFT predicted value in vacuo, 1853 cm^{-1}. This significant result points to the success of DFT calculations in predicting both structural and IR spectroscopic properties for the isolated anion. It also shows that the dielectric continuum model is insufficient to explain the trends in ν(NO) and ν(CN); thus, Table 2 shows that only slight changes are obtained in the calculations for $\epsilon = 35.9$ and 78.5 compared to vacuum; the values are in fact significantly lower compared to the experimental values obtained in acetonitrile and water solutions, respectively. The results for ν(CN) are also disappointing; when going to higher dielectric constants, the ν(CN) values (which are too low), display a reverse trend compared to the one shown by the experimental results.

The decrease in ν(NO) for lower AN can be easily explained on the grounds of the previously quoted specific interactions of cyanides with the solvent.[49,50] Thus, in dipolar aprotic solvents the cyanides become more electron rich and shift electron density into the metal and the π*(NO) orbital, thus lowering ν(NO). A further evidence is given by the shift in the reduction potential of $[Fe(CN)_5NO]^{2-}$ (which measures a charge transfer process essentially located at the nitrosyl ligand) of ca. 0.4 V toward more negative values when going from an aqueous to an acetonitrile solution.[51] This is a consequence of the stronger Fe−NO π-interaction in acetonitrile, which raises the energy of the π*(NO) level. The minor changes in ν(CN) (Table 2, Figure 3) are probably related to compensating electron density effects associated to the removal of charge from the different $\sigma-\pi$ cyanide orbitals (see below). Consistent with this overall picture, the influence of dehydration (Table 2) or the change in countercations should be certainly associated with specific interactions on cyanides, rather than with direct interactions with the nitrosyl ligand.[19,20] In view of the consistent results and interpretation on specific interactions, the failure of DFT-reaction field calculations in accounting for the solvent effects is not unexpected. Previous attempts to find reasonable correlations between ν(MLCT) and different dielectric functions for the series of $Ru(CN)_xL_{6-x}$ complexes were also unsuccessful.[50] However, in addition to the good agreement between theory and experiment for the isolated and poorly interacting anion, respectively, DFT calculations are shown to be useful in predicting or interpreting the experimental data. Thus, the assertion that cyanides but not nitrosyl are mainly interacting with the solvent is confirmed by the partial charges (Table 4), evaluated from the DFT electrostatic potential (Table 3). As expected, the DFT calculation predicts that the N in the nitrosyl is positive (+0.834 e) and the terminal N in the cyanides is negative. According to this charge distribution, and taking into account steric and statistical arguments, the solvent should interact with the terminal N in cyanides and the terminal O in the nitrosyl, but since the charge on the N atoms is −0.72 e (average), while in the O atoms it is only −0.28 e, the preferred interaction will be through the cyanides. As a further confirmation, calculations were performed for the $[Fe(CN)_5NO]^{2-}$ ion solvated with one water molecule; when the latter interacts either with one of the cyanides or with the nitrosyl group, the calculated interaction energies were −14.1 and −5.0 kcal/mol, respectively. Finally, current experimental evidence shows that hydrogen bonds of variable strength are formed between the

(51) Bowden, W. L.; Bonnar, P.; Brown, D. B.; Geiger, W. E., Jr. *Inorg. Chem.* **1977**, *16*, 41.

Table 3. Cyanide and Nitrosyl Orbital Populations[a]

	$\epsilon = 1$	$\epsilon = 35.9$	$\epsilon = 78.5$	prot complex	*a*	*b*	*c*
ν(NO), cm^{-1}	1853	1866	1869	1906	1940	1918	1937
r(NO), Å	1.170	1.164	1.164	1.157	1.125		
σ(NO)	1.731	1.740	1.739	1.687			
π(NO)	4.00	4.00	4.00	4.00			
π*(NO)	1.233	1.174	1.172	1.125			
$\nu(CN)_{eq}$, cm^{-1}	2115	2114	2113	2139	2143	2156	2143
r$(CN)_{eq}$, Å	1.181	1.181	1.182	1.178	1.153		
$\sigma(CN)_{eq}$	1.120	1.126	1.127	1.111			
$\pi(CN)_{eq}$	4.00	4.00	4.00	4.00			
π*$(CN)_{eq}$	0.00	0.00	0.00	0.00			
σ(CN)	1.179	1.180	1.180	1.134			
π(CN)	4.00	4.00	4.00	4.00			
π*(CN)	0.00	0.00	0.00	0.00			
$\nu(CN)_{ax}$, cm^{-1}	2125	2116	2116	2091	2174	2164	2155
r$(CN)_{ax}$, Å	1.180	1.182	1.182	1.175	1.153		
$\sigma(CN)_{ax}$	1.206	1.227	1.229	1.155			
$\pi(CN)_{ax}$	3.920	3.915	3.915	3.828			
π*$(CN)_{ax}$	0.00	0.06	0.06	0.08			

[a] Experimental results for $Na_2[Fe(CN)_5NO]\cdot 2H_2O$, refs 20 and 35. [b] Experimental results for anhydrous $Na_2[Fe(CN)_5NO]$, ref 35. [c] Experimental results for aqueous solution (this work); the values for axial and equatorial cyanides correspond to the observed unresolved band.

Table 4. Partial Charges (au) for $[Fe(CN)_5NO]^{2-}$ in Vacuo

atom	partial charge	atom	partial charge	atom	partial charge
Fe	−2.283	C3	0.660	N3	−0.728
C1	0.702	C3′	0.660	N3′	−0.728
N1	−0.707	N2	−0.730	N4	0.834
C2	0.665	N2′	−0.730	O1	−0.280
C2′	0.665				

N-end of cyanides with water[52] (or oxonium ions)[47] acting as acceptors; crystallographic data also show that this is not the case regarding the nitrosyl ligand.[29]

Table 3 shows DFT calculations on cyanide and nitrosyl orbital populations. When going from vacuum to $\epsilon = 78.5$, the σ(NO) and π(NO) orbital populations remain constant but a significant decrease in π*(NO) is obtained. This is in agreement with the calculated trends in ν(NO), as well as in the bond equilibrium distances, consistent with a stronger and shorter bond, respectively.

The changes in σ(CN), π(CN), and π*(CN) orbital populations are not significant for equatorial cyanides; for the axial cyanide, compensating changes seem to be operative: the calculations show an increase in σ(CN) and π*(CN) populations; as seen in Table 2, the ν(CN) values show a decreasing trend, suggesting a predominance of electron transfer through the π framework. In view of the previously quoted limitations of the continuum model, these calculations should be interpreted with caution; in fact, as shown above, experimental trends in ν(CN) show a slight increase when going from vacuum to water, in contrast to the DFT-reaction field predictions.

As a simple model for a strong acceptor, we also performed calculations with the complex protonated at the cyanide group trans to the NO. From the results shown in Table 3 it can be seen that the calculated ν(NO) value is expectedly the highest among the previously calculated ones, in agreement with a strong specific interaction at the axial cyanide. Consistently, the π*(NO) orbital population is the lowest, compensating for the decrease in the σ(NO) orbital population. The calculated shifts for the equatorial cyanides are reasonably close to the experimental value for the solid hydrated salt, but the changes in ν(CN) for the axial cyanide show a significant decrease, to 2091 cm^{-1}, expectedly associated with a removal of charge from the σ(CN) orbital and an increase in the π*(CN) orbital populations. This result seems to be the consequence of protonation, but it does not account for the real experimental value for $\nu(CN)_{ax}$ in the solid. Therefore, this calculation should be taken as a crude model for probing the role of specific interactions, because the latter are not simply related to the protonation of one cyanide ligand. In fact, $\nu(CN)_{ax}$ for the solid dihydrate was assigned at 2174 cm^{-1},[35] which is significantly higher than the average $\nu(CN)_{eq}$ values, ca. 2150 cm^{-1}. The electron-withdrawing influence of nitrosyl shows to be operative on all the cyanide ligands but is particularly enhanced at the trans CN group, seemingly because the electronic shifts are propagated through the π*(CN)−Fe−π*(NO) framework.[18]

Conclusions

The shifts in the absorption bands for the UV−visible and IR spectra of $[Fe(CN)_5NO]^{2-}$ in different solvents demonstrate that specific interactions are operative between the donor cyanide ligands and the acceptor solvents. A very sensitive probe of the interaction is given by shifts in ν(NO), which decreases for lower acceptor solvents. In the limit of negligible acceptor influence, the experimental results agree fairly well with the predicted DFT values (structural parameters and vibrational wavenumbers) for the isolated species. However, calculated values for the anion immersed in different continuum media do not agree with experiment, as expected, showing the failure of dielectric continuum models in explaining the experimental results. By performing DFT calculations with a species protonated at a cyanide (trans to the NO), a crude model system for specific interactions is obtained. Thus, a realistic (but expensive) approach should consider the use of supermolecule or coupled quantum−classical methodologies.[53]

On the other hand, referring to the problem raised in the Introduction, it has been noted that the metal−NO^+ carriers are susceptible to nucleophilic attack by several bases under physiological conditions.[54] It has been shown that the rate of these addition reactions depends on the pH, redox environment, and molecular structure of the nitrosyl carrier, as well as on the nucleophilic reactant, which can be mainly mercaptide or ammine species in the relevant biological fluids. By studying

(52) Holzbecher, M.; Knop, O.; Falk, M. *Can. J. Chem.* **1971**, *49*, 1413.

(53) (a) Field, M. J.; Bash, P. A.; Karplus, M. *J. Comput. Chem.* **1990**, *11*, 700. (b) Estrin, D. A.; Liu, L.; Singer, S. J. *J. Phys. Chem.* **1992**, *96*, 5325.

(54) (a) Stamler, J. S.; Simon, D. I.; Osborne, J. A.; Mullins, M. E.; Jaraki, O.; Michel, T.; Singel, D. J.; Loscalzo, J. *Proc. Natl. Acad. Sci. U.S.A.* **1992**, *89*, 444. (b) Stamler, J. S. *Cell* **1994**, *78*, 931.

the reactivity of several nitrosyl complexes with nucleophiles, it was shown that the rates are particularly sensitive to ν(NO).[55] The latter depends obviously on the bonding ability of the coligands in the first coordination sphere, but the present work shows that the second coordination sphere also shows noticeable effects.

The heme-type enzymes are well-known targets for NO binding and further reactivity,[54] and it seems highly feasible that changes in the structure of the protein, associated with the introduction or removal of hydrophobic groups, could affect the local environment and influence the nitrosyl electron density, thus establishing a mechanism for a regulatory action.

Acknowledgment. This investigation was partially supported by the Regione Autonoma della Sardegna and by the University of Buenos Aires. D.A.E. and L.D.S. acknowledge the support of Secretaría de Ciencia y Técnica (Universidad de Buenos Aires). D.A.E. acknowledges Fundación Antorchas (Argentina) for financial support. D.A.E. and J.A.O. are members of the scientific staff of CONICET (National Scientific Council, Argentina).

IC951202C

(55) Bottomley, F. *Acc. Chem. Res.* **1978**, *11*, 158.